Physics and Imaging in Radiation Oncology 8 (2018) 44–50

Contents lists available at ScienceDirect

Physics and Imaging in Radiation Oncology

journal homepage: www.elsevier.com/locate/phro

Original Research Article

Skin dose calculation during radiotherapy of head and neck cancer using deformable image registration of planning and mega-voltage computed tomography scans

Marco Branchini[a], Sara Broggi[a], Italo Dell'Oca[b], Giovanni Mauro Cattaneo[a], Riccardo Calandrino[a], Nadia Gisella Di Muzio[b], Claudio Fiorino[a,*]

[a] Department of Medical Physics, San Raffaele Scientific Institute, Milano, Italy
[b] Department of Radiotherapy, San Raffaele Scientific Institute, Milano, Italy

ARTICLE INFO

Keywords:
Skin dose
DIR
MVCT
Dose of the day
Tomotherapy

ABSTRACT

Background and Purpose: Head-Neck (HN) patients may experience severe acute skin complications that can cause treatment interruption and increase the risk of late fibrosis. This study assessed a method for accurately monitoring skin dose changes during helical tomotherapy for HN cancer based on deformable image registration of planning computed tomography (CT) and mega-voltage CT (MVCT).

Materials and Methods: Planning CTs of nine patients were deformably registered to mid-treatment MVCT (MV15) images resulting in CTdef images. The original plans were recalculated on both CTdef and mid-treatment kilo-voltage CT (CT15) taken as ground truth. Superficial layers (SL) of the body with thicknesses of 2, 3 and 5 mm (SL2, SL3, SL5) were considered as derma surrogates. SL V95%, V97%, V98%, V100%, V102%, V105% and V107% of the prescribed PTV dose were extracted for CT15/CTdef and compared (considering patients with skin dose > 95%). For comparison, doses were calculated directly on the calibrated MVCT and analyzed in the same way.

Results: Differences between SL2/SL3/SL5 V95%-V107% in CT15/CTdef were very small: for eight of nine patients the difference between the considered SL2 Vd% computed on CTdef and CT15 was less than 1.4 cm^3 for all d%. A larger value was found when using MVCT for skin dose calculation (4.8 cm^3 for SL2), although CTdef body contour matched CT15 body with accuracy similar to that of MV15.

Conclusions: Deforming the planning CT-to-MVCT was shown to be accurate considering external body contours and skin DVHs. The method was able to accurately identify superficial overdosing.

1. Introduction

Malignant tumours of Head-Neck (HN) constitute around 3.8% of all cancers worldwide; they rank as the seventh most frequent type of tumour by incidence, and the ninth most common cause of cancer death [1]. Radiotherapy is a common treatment modality for these malignancies, often in combination with chemotherapy. Nevertheless, avoidance of radiation-induced side effects is critical, due to both the presence of numerous organs at risk (OARs) and significant patient anatomical variations that may occur during treatment [2–4]. For this purpose, Intensity Modulated Radiation Therapy (IMRT) is widely used to reduce toxicity thanks to superior dose conformation to the Planning Target Volume (PTV); combination with Image Guided Radiotherapy (IGRT) assures correct patient set-up, with the possibility of incorporating anatomical changes during treatment by means of Adaptive Radiotherapy (ART) [2,5–9]. Despite these improvements, HN patients still experience severe complications, two of the most frequent being xerostomia and mucositis [3,10]. In recent years, several authors have focused attention also on skin toxicity [11–14]. Indeed, HN patients may experience severe acute skin complications that can cause treatment interruption and increase the risk of late fibrosis [15]. More specifically, skin complications were reported as frequent in patients treated with Helical Tomotherapy (HT) [16]: very interestingly, an incidence approximately three times that of volumetric modulated arc therapy was recently reported by a French National consortium in a large group of patients treated with the same clinical protocol [17].

In-room imaging may be exploited also to compute patients' daily dose distribution ("dose of the day") with the aim of monitoring the

* Corresponding author at: Medical Physics Department, San Raffaele Scientific Institute, Via Olgettina 60, 20132 Milano, MI, Italy.
E-mail address: fiorino.claudio@hsr.it (C. Fiorino).

https://doi.org/10.1016/j.phro.2018.11.008
Received 7 March 2018; Received in revised form 21 November 2018; Accepted 22 November 2018

treatment and facilitating the evaluation of the need for and timing of re-planning [18–20]. Various methods have been proposed for dose of the day calculation. Direct dose calculation on Cone Beam Computed Tomography (CBCT) and Megavolt Computed Tomography (MVCT) images is capable of good dosimetric accuracy, but requires specific and frequent calibrations [21–25]. Furthermore, MVCT provides poor contrast for soft tissue imaging [26] in comparison with CT and CBCT. Thus, the development of alternative methods for combining up-to-date, on-board anatomy information and better soft tissue definition is of interest. Various methods based on Deformable Image Registration (DIR) between planning CT and CBCT/MVCT daily images have been proposed to this end. These methods have the advantages of producing images with higher soft tissue contrast than CBCT or MVCT, and without the need for specific image value-density tables or tissue segmentation for dose computation, while resulting in comparable or superior dosimetric accuracy [19,27].

In a previous study [27], the validation of a DIR-based method for dose of the day calculation in HT was presented with a particular focus on dosimetric accuracy. In the current work, a DIR-based method based on a different DIR algorithm was analyzed with the specific aim of assessing whether this method is suitable for the accurate monitoring of skin dose changes during treatment, and thus, if it could be considered for skin-sparing treatment adaptation.

2. Materials and methods

At our institution, HN patients are treated with HT [28]. Most patients are treated following an institutional protocol consisting of a Simultaneous Integrated Boost (SIB) scheme delivering 54/66/69 Gy in 30 fractions, to low-risk lymph nodes (PTV1), tumour and positive lymph nodes (PTV2) and FDG-PET positive volumes respectively [29]. A sample of ten consecutive HN patients was here analyzed: eight patients were treated with SIB and two with a sequential scheme delivering 54 Gy to PTV1 followed by a boost to PTV2 (70.2 Gy), with a daily dose of 1.8 Gy/fr.

A DIR approach was implemented to compute the dose of the day by using the constrained intensity-based DIR algorithm of the commercial software MIM (Cleveland, Ohio): the planning CT (CTplan) was deformably registered to the MVCT corresponding to the 15th fraction (MV15) resulting in a deformed image (CTdef), and the original plan was employed to recalculate the dose on CTdef. To assess the geometric and dosimetric accuracy of the proposed method, a diagnostic kilovoltage CT (CT15) was specifically acquired-on the same day as MV15 with same patient set-up, and the original plan was recalculated on CT15 in the same way as for CTdef. CT15 was considered as ground truth and taken as reference for the assessment of the method. Details of the imaging protocols employed are described elsewhere [27].

2.1. Deformable image registration

In order to decrease MVCT image noise while preserving sharp edges for tissues with different densities, a gradient anisotropical diffusion filter was applied to MVCTs, as proposed by Lu et al. [30]. This filtering was performed with the "Gradient Anisotropic Diffusion" tool of 3D-Slicer (Insight Toolkit) [31]. Subsequently, for each patient a CTplan was first rigidly registered to MV15 employing MIMfusion, the rigid registration MIM tool, which uses mutual information (MI) as similarity metric. The rigid registration was then refined with the "Box-Based Assisted Alignment" rigid registration tool focusing on spinal column matching. Starting from the rigidly registered CTplan, the deformable registration was performed by the MIM tool "VoxAlign Deformation Engine" using constrained intensity-based deformable registration, with the deformable smoothness factor (DSF) value set to 2.0, resulting in CTdef. The accuracy of this method has been demonstrated in intra modality or CT-to-CBCT registrations [32–34]. CT15 was rigidly registered with CTdef through MIMfusion taking CT15 as moving image to minimize any slight positioning differences. The resulting images were saved in DICOM format and made square by adding a band of black voxels with a Matlab script, given that squared images are mandatory for dose computation in the Tomotherapy system.

2.2. Dose computation

In order the recalculate the original plan, registered CTdefs and CT15s were imported into the DQA (dosimetry quality assurance, TomoHD System, DQA Station 5.1.0.4, Accuray Incorporated, Sunnyvale, CA) Station module of the HT planning system (where only manual registrations are possible) as "phantoms" for QA, and the "Tomo" couch was added. In order to properly recalculate the dose, CT15 was manually registered to CTplan and CTdef to CTplan separately, matching external markers and spine anatomy with the overlaid CTplan structures. Sinograms of the original HT were then recalculated on both CTdef and CT15 with fine resolution grid ($0.15 \times 0.15\,cm^2$) and the resulting doses were exported with images from the DQA Station for geometric and dosimetric analyses.

2.3. Overall dosimetric accuracy analysis

Geometrical accuracy of DIR methods was first assessed qualitatively in order to check for evident inconsistencies generated in CTdef images. To compare the dose distributions recalculated on CTdef and CT15, 3D global gamma index [35] analyses (2%-2 mm, threshold 10% of the global maximum) were then performed for points inside CT15 body using Slicer RT (3D Slicer software platform, version 4.0.5-1) [36]. A rigid registration was performed in Slicer RT between the two dose distributions (by moving CTdef dose distribution). This last step was performed in order to minimize manual rigid registration errors in the DQA Station module. Moreover, Dose Differences (DD), computed with MapCheck SNC Patient software (SunNuclear Corporation, Melbourne, United States) were performed for all patients in a similar way as described in [27] where DIRs were performed with a 3D Slicer tool using MI as similarity metric.

2.4. Validation of the method for skin dose computation

To validate the use of DIR for computing the dose of the day in superficial body layers, we analyzed DVHs of inner body rings with thicknesses of 2, 3 and 5 mm taken as surrogates of derma and contoured on CTdef and CT15. In particular, body contour was automatically segmented with MIM by the "Whole Body" contouring tool and inner rings were constructed using the "Expand/Contract Contour" tool. The cranial-caudal extensions of these external rings were defined corresponding to the high–dose PTV extension (PTV2). DVHs of the inner rings were calculated in MIM and exported for analysis.

We focused on the ability of the method to assess skin dose distributions with the main aim of investigating whether the "high-dose" skin regions of CT15 dose distributions were in agreement with the corresponding CTdef values. The external layer DVHs V95%, V97%, V98%, V100%, V102%, V105% and V107% of the prescribed PTV2 dose (66 Gy/30 fractions) were extracted for both CT15 and CTdef. One patient with a central PTV2, resulting in a skin dose much lower than 95%, was excluded from the analysis, thus reducing the number of patients considered for the validation of the skin dose application to nine. For V95–V107%, the linear correlation between the corresponding absolute volume estimated with CT15 and CTdef was evaluated: R^2 values of the corresponding linear plots and Spearman's rank correlation coefficients were used to quantify correlations. To estimate the 90% confidence level of the agreement between the skin dose calculated on CT15 and CTdef, the absolute difference value between Vd% of CTdef and CT15 for which eight of nine patients were in agreement for each considered dose d% was taken (disregarding the largest value of the difference).

To test whether CTdef can detect dose changes according to CT15, for each patient, the difference between CT15 and CTplan DVHs was compared against the difference between CTdef and CTplan DVHs. Because skin dose monitoring should be more important for the SIB technique due to higher dose/fraction, this analysis was focused on the seven patients treated with SIB fractionation and superficial dose > 95%. Mean changes from planning values of V95%–V107% were also considered.

In order to assess whether the assumption of using CT15 as ground truth for skin dose computation employing the proposed DIR method is sufficiently accurate, the surface-to-surface (unsigned) distance between CT15 and CTdef body contours (along PTV2 extension) was calculated with the RayStation software platform (ver. 7, RaySearch Laboratories, Stockholm, Sweden) considering CT15 contours as gold standard. In particular, a surface ROI was constructed by expanding/contracting CT15 body by 0.3 mm, thus defining a 0.6 mm thick layer (CT15 surface). This allowed us to consider for the analysis only points near the skin surrounding the head-neck, while excluding the transversal surfaces at the cranio-caudal extremities of the ROI. The choice of expanding/contracting by 0.3 mm was dependent on the capability of RayStation to correctly construct a continuous layer with thicknesses equal to or larger than 0.3 mm in axial slices, and by the need for a symmetric expansion/contraction around the CT15 external surface to calculate distances accurately. Thus, in analyzing images exported from the DQA Station, the resulting differences of external surface definitions deriving from all possible sources of error (differences in patient positioning, precise body contour definition in MVCT image, deformable image registration in MIM, manual rigid registrations in DQA Station and automatic body segmentation) between CT15 and CTdef were taken into account.

2.5. Comparison with skin dose computed on MVCT

To assess whether a difference in superficial dose calculation accuracy was present when using CTdef in place of a direct dose calculation on MVCT, the original (unfiltered) MV15s were employed for dose calculation considering the HU-to-density table measured in the trimester of each treatment. Similarly to CT15s and CTdefs, MV15s were imported into the DQA Station and manually registered (rigidly) to the CTplan. Inner rings were defined and analyzed as above. Differences between the considered Vd% calculated on MVCT and CTdef were compared by means of Wilcoxon rank sum tests for paired samples, with a p-value of 0.05 or lower considered statistically significant.

As before, in order to quantify external differences of body surface definition between CT15 and MV15, both with same PTV2 extension, surface-to-surface distances were evaluated as described for CT15-to-CTdef surfaces distance. Furthermore, the geometrical similarity between body contours of CTdef and MV15 (exported from the DQA Station) was analyzed by calculating the surface-to-surface distance within PTV2 extension as described above. In this case, a 0.6 mm thick layer was defined by expanding/contracting the CTdef body taken as reference. The differences with respect to CT15 body surfaces between CTdef and MVCT were tested by the Wilcoxon rank sum test. Statistical tests were performed with RStudio software, version 1.1.447 (RStudio, Boston, USA).

3. Results

3.1. Overall dosimetric accuracy analysis

When examining the subtraction images of CT15 and CTdef (Fig. 1), neither the current method nor the 3D-Slicer DIR method previously analyzed by our group demonstrated a clear superiority. Accurate matching of the body contour between the deformed image and MV15 was achieved with both methods, although some inconsistencies were observed at the level of the shoulders (Fig. 1). Dosimetric accuracy was analyzed both slice by slice and volumetrically (Table 1): 88% ± 1% of the voxels had a dose difference less than 2% (of the maximum dose value in each slice), and 95.0% ± 0.7% of body voxels passed the global 3D gamma analysis (2%/2 mm, considering a dose threshold of 10% of the global maximum).

3.2. Validation of the method for skin dose computation

DVHs of the inner body rings of 2, 3 and 5 mm for CT15 and CTdef are shown in Fig. 2: for all patients considered, only small differences were present. A very high correlation between external layers DVHs estimated on CT15 and CTdef was found by comparing V95%–V107% (Table 2 and Supplementary Material): the average value of R^2 values

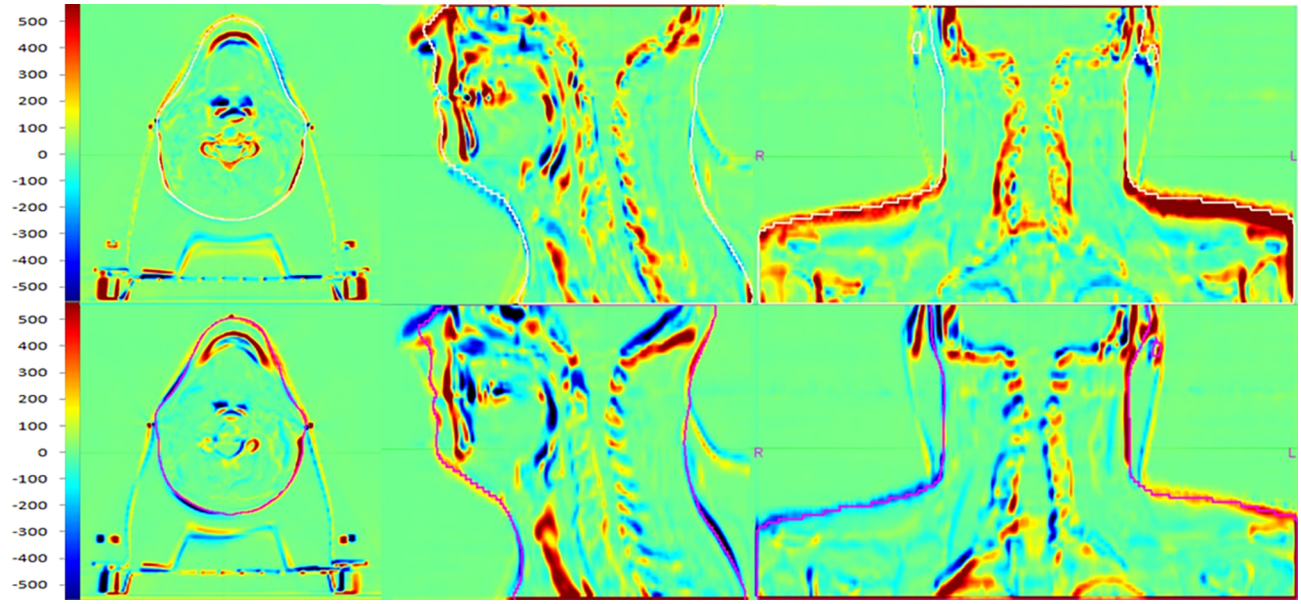

Fig. 1. subtraction images in HU scale of CT15 and CTdef for patient 2 with highlighted CT15 body contour for the proposed method (above) and for 3D-Slicer method, whose analysis was presented in [19]. MIM produces the largest inaccuracies at the level of the shoulders; elsewhere results are generally acceptable.

Table 1
Average 3D gamma (2%/2 mm, threshold 10%) pass-percentages in CT15 body and 2D DD2% pass-percentages considering slices with maximum > 10% of the prescribed dose.

Patient	3D γ (2%/2 mm)	ΔD < 2%
1	93.5	87.3 ± 0.9
2	93.0	87.7 ± 0.9
3	96.4	90.1 ± 0.1
4	96.6	79.6 ± 1.1
5	95.0	89.1 ± 1.1
6	96.9	89.9 ± 0.7
7	90.4	81.7 ± 2.6
8	94.0	91.6 ± 0.7
9	97.0	91.0 ± 0.6
10	97.2	91.0 ± 0.4
Mean	95.0 ± 0.7	87.9 ± 1.3

was 0.91, while the Spearman rank test showed that five Vd% of the seven analyzed were significantly correlated (p-values < 0.05) between CT15 and CTdef for the 2 mm layer structures, and six of seven for the 3 mm layer structures. When considering the absolute differences between V95% and V107% on CTdef against CT15, the maximum deviations in the 2 mm inner body ring was -2.6 cm^3. The suggested 90% confidence level was found to range between 0.0 cm^3 and 1.4 cm^3 for the 2 mm layer at different d%, with an average value of approximately 0.6 considering all d% (Fig. 3) and approximately 0.8 cm^3 if excluding V105%–V107%.

Interestingly, differences between the CT15-CTplan and the CTdef-CTplan were also very small (Supplementary Material). For one patient diagnosed with base of tongue carcinoma showing a significantly higher delivered skin dose (CT15) compared to the planned skin dose, this radiotherapy induced change was consistently detected also on CTdef (Supplementary Material). Of the seven patients treated with SIB technique, one patient received an increase in skin dose relative to planned dose with at least one ΔVd% > 1.4 cm^3 for the considered DVH points, while two patients showed a decrease in skin dose with at least one ΔVd% < −1.4 cm^3. The other patients presented absolute skin Vd % variations smaller than 1.0 cm^3.

CTdef body contour matched CT15 body with good accuracy. In fact, the average value of the mean distances between CT15 and CTdef external surfaces was 0.28 ± 0.21 cm (mean ± one SD), whereas the median value was 0.16 cm (Fig. 4).

3.3. Comparison with skin dose computed on MVCT

Computing the dose directly on calibrated MVCT resulted in lower accuracy than when using CTdef. The estimation of the 90% confidence level was carried out in the same way as for CTdef, and ranged between 0.2 and 4.8 cm^3 for the 2 mm layer at different d% with an average value of 1.9 cm^3 for the 2 mm layer considering all d% and 2.6 cm^3

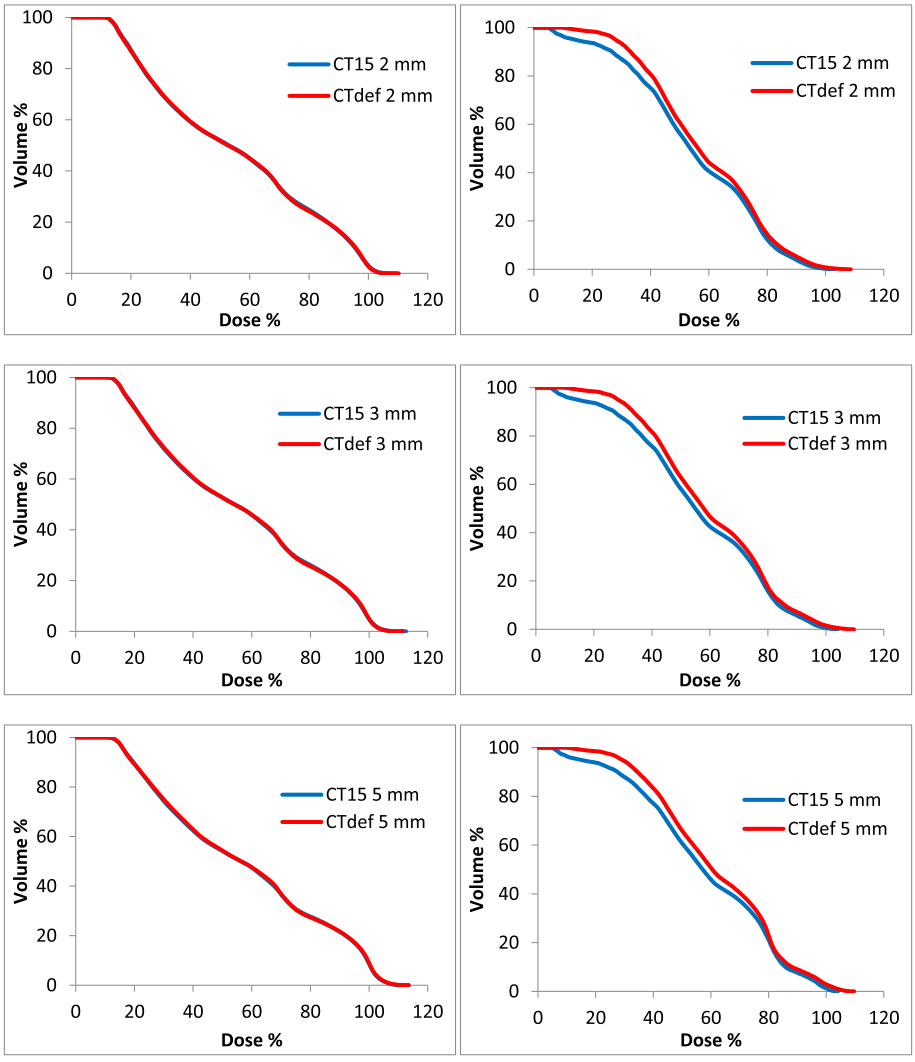

Fig. 2. DVHs of 2 mm, 3 mm and 5 mm layers (from top to bottom) for the patient with best results (left) and with worst results (right).

Table 2
R^2 values for trendlines of fixed dose DVH points for CT15 and CTdef DVH of external layers. *Spearman rank test p-values < 0.05.

Percent of dose (%)	2 mm layer R^2	3 mm layer R^2	5 mm layer R^2
95	0.97*	0.98*	0.99*
97	0.95*	0.97*	0.98*
98	0.93*	0.96*	0.98
100	0.89*	0.94*	0.96
102	0.80*	0.88*	0.93
105	0.83	0.83	0.87
107	0.83	0.86*	0.77*

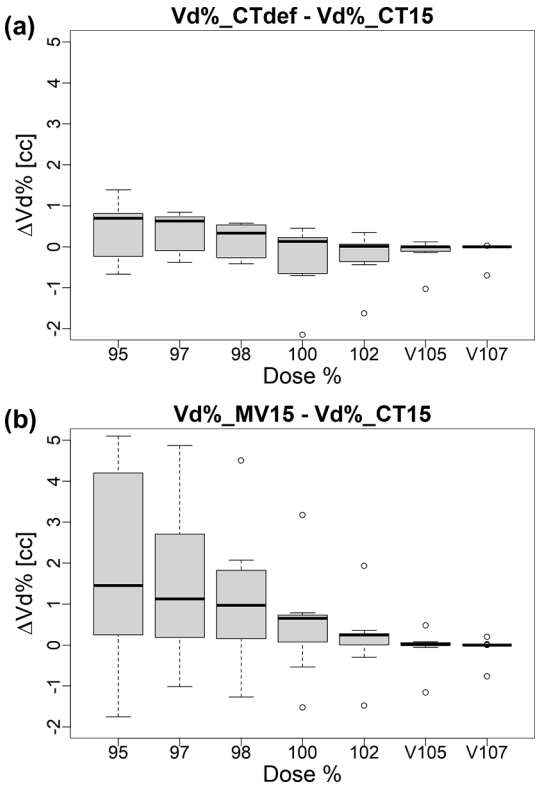

Fig. 3. Boxplot of the difference between Vd% calculated on CTdef and CT15 (a) at each considered dose d% for 2 mm external layers and corresponding boxplot for MV15 (b).

excluding V105%–V107% (Fig. 3). The differences between CTdef and MVCT were statistically significant (Wilcoxon test) for all Vd% except V105% and V107%.

Of note, the average distance from CT15 to MV15 body surfaces was very similar to that from CT15 to CTdef (0.26 ± 0.15 cm vs 0.28 ± 0.21 cm, respectively) demonstrating that the geometric mismatch between CT15/CTdef and CT15/MV15 is comparable (Fig. 4). In fact, the differences between CTdef-to-CT15 and MV15-to-CT15 surface distances for each patient were very small (0.5 ± 0.5 mm), and not statistically significant (Wilcoxon test). This result was confirmed also by the analysis of the corresponding surface-to-surface distance between CTdef and MV15, with an average value of 1.5 ± 0.7 mm (Fig. 4).

4. Discussion

The development and validation of a method to accurately calculate the skin dose of the day delivered in HT of HN patients was investigated. To our knowledge, this is the first study to assess the

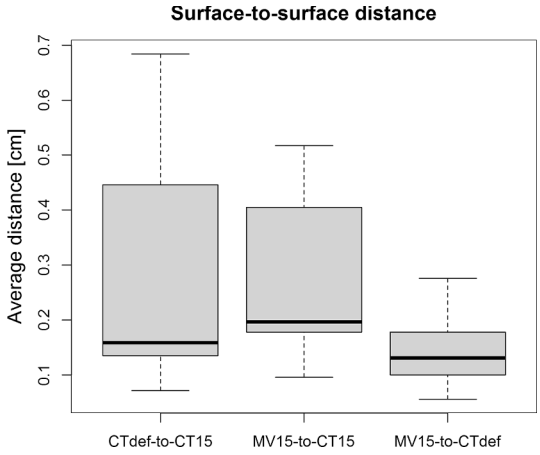

Fig. 4. Boxplot of the surface-to-surface distance between CTdef and CT15, MV15 and CT15, MV15 and CTdef.

accuracy of a method to monitor skin dose during radiotherapy treatment and validate its use for potential skin-sparing adaptive applications.

Through DIR of the planning CT to daily MVCT, a synthetic CT can be generated and dose can be calculated upon it without the need for frequent Image Value to Density table calibration of MVCTs. Deformable registration results were consistent and qualitatively good for body contour matching, despite the fact that, on rare occasions, images showed some artificial “fluidity”, especially in the shoulder region, probably due to loose regularization strength of the algorithm. For this reason, a higher than default value was used for the deformable smoothness factor (DSF) of the MIM constrained-intensity based DIR algorithm; increasing this parameter even further did not substantially affect the results (data not shown).

The overall dosimetric agreement (CTdef vs CT15) showed a fraction of body voxels with gamma 2%/2 mm ≤ 1 of 95.0% ± 0.7%. Thus, from the point of view of dose of the day calculation, the method presented an accuracy comparable to that using standard kVCT. Shoulder contraction due to limited MVCT FOV was present in CTdef images, as reported also for the 3D-Slicer software [27], but does not significantly affect the gamma test, as the shoulders are routinely blocked during plan optimization and delivery. The passing rates of γ(2%, 2 mm) and DD2% found in our study are similar to those reported by Veiga et al. [19], where the planning CT was deformably registered to on-board CBCT (97.1% ± 1.1% and 90.0 ± 0.9%), as well as to those found in a preliminary study by our group [27] when using 3D-Slicer for planning CT-to-MVCT DIR (94.6% ± 0.8% and 87.9% ± 1.2%) or directly computing the dose on calibrated MVCT (95.7% ± 0.4% of voxel passing γ test).

The Tomotherapy dose calculation algorithm is the collapsed cone convolution model, whose accuracy in calculating skin dose in the head and neck region has been previously reported [37–41]. Other studies have also confirmed its accuracy, although relatively small overestimates have been noted [42–46]. In this work, the feasibility of skin dose monitoring during HT was focused upon: the DIR-based method was found to be very promising in the challenging application of capturing a possible overdosing of the first few mm from the body surface. Differences between CT15 and CTdef < 1.4 cm^3 for at least eight of nine patients at each dose d% were found for the 2 mm body layer in a typical HN patient population. This value corresponds to a minor fraction of the SL2 volumes that range from 52.7 to 241.3 cm^3 (average value 116.3 ± 58.7 cm^3). This is remarkable, considering that a 5 mm positioning error could result in an impact of from −3% to +9% on surface dose [47]. We thus suggest that the method may be used with a high level of confidence to track Vd% changes larger than approximately 1.4 cm^3 or, equivalently, to a skin surface of 7 cm^2.

The DIR method was also compared against the direct skin dose calculation method using calibrated MVCTs. It is interesting that skin dose calculated on MV15 was found to be less accurate than that calculated on CTdef with a reasonable lowest detectable shift from planning CT of 4.8 cm^3 versus 1.4 cm^3 when using CTdef. This result represents added value in using DIR for precise skin dose assessment during treatment.

A thorough geometric analysis of the distance between CTdef and MVCT body surfaces demonstrated that the DIR method employed is accurate in reproducing updated body contours with average errors lower than 1.5 mm and a standard deviation of 0.7 mm. This is remarkable, considering the gross mismatch in body contours when the CTdef and MVCT were rigidly aligned to CTplan in the DQA station. The largest errors were found in the shoulder region, where strict patient immobilization is more difficult, but as noted previously, this should not affect dose distributions significantly, given the use of planning blocks.

The assumption of using CT15 as ground truth has been assessed by means of a surface-to-surface distance analysis with CTdef/MV15. The average distances of 2.8 ± 2.1/2.6 ± 1.5 mm can be considered a good result, especially considering that for each patient the average body surface distances CT15-CTdef and CT15-MV15 were very close (0.5 ± 0.5 mm), and that the experimental setting reproduces real patient positioning during treatment. This result suggests that dosimetric errors are probably inherent to dose computation on MVCT images rather than geometric mismatches between CT15 and MV15 body contours. Future work will be aimed at a detailed investigation of MVCT air-body interface definition.

This study presents certain limitations: the number of patients considered is limited, and different MV15 voxel sizes and different CT15/MV15 slice thicknesses were considered. In particular, voxel size and slice thickness could impact on dose computation. Nonetheless, the study provides a thorough validation of the method for skin dose calculation using DIR and MVCT in a typical group of HN patients.

Having completed the validation of the methodology to compute skin dose of the day, the proposed method was employed in a monitoring analysis of skin dose during treatment on a larger number of HN patients. This analysis was recently completed and is the focus of a more specific work. In particular, the selection of the patients who could benefit from re-planning and the determination of skin dose constraints for the prevention of skin complication has been carefully investigated.

In conclusion, a CT-plan-to-MVCT DIR-based methodology for skin dose of the day monitoring in HT of Head Neck has been assessed, showing satisfactory results regarding the dosimetric and geometric accuracy of the method. A limiting value of 1.4 cm^3 was reasonably suggested as minimum detectable volume shift from planned DVH in the range of 95–107% of the prescribed PTV dose. Planning CT-to-daily MVCT DIR can thus be reliably used to inform adaptive skin-sparing procedures for HN patients.

Conflict of interest

The authors have no conflicts of interest to disclose.

Acknowledgments

The project was supported in part by an Associazione Italiana per la Ricerca sul Cancro (AIRC) grant (IG18965).

Appendix A. Supplementary material

Supplementary data to this article can be found online at https://doi.org/10.1016/j.phro.2018.11.008.

References

[1] World Cancer Report 2014. International Agency for Cancer Research: WHO; 2014.
[2] Veresezan O, Troussier I, Lacout A, Kreps S, Maillard S, Toulemonde A, et al. Adaptive radiation therapy in head and neck cancer for clinical. Jpn J Radiol 2016;2:43–52.
[3] Hunter KU, Fernandes LL, Vineberg KA, McShan D, Antonuk AE, Cornwall C, et al. Parotid glands dose-effect relationships based on their actually delivered doses: implications for adaptive replanning in radiation therapy of head-and-neck cancer. Int J Radiat Oncol Biol Phys 2013;87:676–82.
[4] Lee C, Langen KM, Lu W, Haimerl J, Schnarr E, Ruchala KJ, et al. Assessment of parotid gland dose changes during head and neck cancer radiotherapy using daily megavoltage computed tomography and deformable image registration. Int J Radiat Oncol Biol Phys 2008;71:1563–71.
[5] Surucu M, Shah KK, Roeske JC, Choi M, Small Jr W, Emami B. Adaptive radiotherapy for head and neck cancer. Technol Cancer Res Treat 2017;16:218–23.
[6] Castadot P, Lee JA, Geets X, Grégoire V. Adaptive radiotherapy of head and neck cancer. Semin Radiat Oncol 2010;20:84–93.
[7] Deasy JO, Moiseenko V, Marks L, Chao KS, Nam J, Eisbruch A. Radiotherapy dose-volume effect on salivary gland function. Int J Radiat Oncol Biol Phys 2010;76:58–63.
[8] Nutting CM, Morden JP, Harrington KJ, Urbano TG, Bhide SA, Clark C, et al. Parotid-sparing intensity modulated versus conventional radiotherapy in head and neck cancer (PARSPORT): a phase 3 multicentre randomised controlled trial. Lancet Oncol 2011;12(127–36):6.
[9] Marta GN, Silva V, de Andrade Carvalho H, de Arruda FF, Hanna SA, Gadia R, et al. Intensity modulated radiation therapy for head and neck cancer: systematic review and meta-analysis. Radiother Oncol 2014;110:9–15.
[10] De Sanctis V, Bossi P, Sanguineti G, Trippa F, Ferrari D, Bacigalupo A, et al. Mucositis in head and neck cancer patients treated with radiotherapy and systemic therapies: literature review and consensus statements. Crit Rev Oncol Hematol 2016;100:147–66.
[11] Lee N, Chuang C, Quivey JM, Phillips TL, Akazawa P, Verhey LJ, et al. Skin toxicity due to intensity-modulated radiotherapy for head-and-neck carcinoma. Int J Radiat Oncol Biol Phys 2002;53:630–7.
[12] Bonomo P, Loi M, Desideri I, Olmetto E, Delli Paoli C, Terziani F, et al. Incidence of skin toxicity in squamous cell carcinoma of the head and neck treated with radiotherapy and cetuximab: a systematic review. Crit Rev Oncol/Hematol 2017;120:98–110.
[13] Radaideh KM, Matalqah LM. Predictors of radiation-induced skin toxicity in nasopharyngeal cancer patients treated by intensity-modulated radiation therapy: a prospective study. J Radiother Pract 2016;15:276–82.
[14] Bernier J, Russi EG, Homey B, Merlano MC, Mesía R, Peyrade F, et al. Management of radiation dermatitis in patients receiving cetuximab and radiotherapy for locally advanced squamous cell carcinoma of the head and neck: proposals for a revised grading system and consensus management guidelines. Ann Oncol 2011;22:2191–200.
[15] Nevens D, Duprez F, Daisne JF, Laenen A, De Neve W, Nuyts S. Radiotherapy induced dermatitis is a strong predictor for late fibrosis in head and neck cancer. The development of predictive model for late fibrosis. Radiother Oncol 2017;122:212–7.
[16] Kodaira T, Tomita N, Tachibana H, Nakamura T, Nakahara R, Inokuchi H, et al. Aichi cancer center initial experience of intensity modulated radiation therapy for nasopharyngeal cancer using helical tomotherapy. Int J Radiat Oncol Biol Phys 2009;73:1129–34.
[17] Bibault JE, Dussart S, Pommier P, Morelle M, Huguet M, Boisselier P, et al. Clinical outcomes of several IMRT techniques for patients with head and neck cancer: a propensity score-weighted analysis. Int J Radiat Oncol Biol Phys 2017;99:929–37.
[18] Nassef M, Simon A, Cazoulat G, Duménil A, Blay C, Lafond C, et al. Quantification of dose uncertainties in cumulated dose estimation compared to planned dose in prostate IMRT. Radiother Oncol 2016;119:129–36.
[19] Veiga C, McClelland J, Moinuddin S, Lourenço A, Ricketts K, Annkah J, et al. Toward adaptive radiotherapy for head and neck patients: feasibility study on using CT-to-CBCT deformable registration for “dose of the day” calculations. Med Phys 2014;41:031703.
[20] Brown E, Owen R, Harden F, Mengersen K, Oestreich K, Houghton W, et al. Head and neck adaptive radiotherapy: predicting the time to replan. Asia Pac J Clin Oncol 2016;12:460–7.
[21] Yoo S, Yin F-F. Dosimetric feasibility of cone-beam ct-based treatment planning compared to ct-based treatment planning. Int J Radiat Oncol Biol Phys 2006;66:1553–61.
[22] Richter A, Hu Q, Steglich D, Baier K, Wilbert J, Guckenberger M, et al. Investigation of the usability of conebeam CT data sets for dose calculation. Radiat Oncol 2008;3:42.
[23] Dunlop A, McQuaid D, Nill S, Murray J, Poludniowski G, Hansen VN, et al. Comparison of CT number calibration techniques for CBCT based dose calculation. Strahlenther Onkol 2015;191:970–8.
[24] Langen KM, Papanikolaou N, Balog J, Crilly R, Followill D, Goddu SM, et al. QA for helical tomotherapy: report of the AAPM Task Group 148. Med Phys 2010;37:4817–53.
[25] Langen KM, Meeks SL, Poole DO, Wagner TH, Willoughby TR, Kupelian PA, et al. The use of megavoltage CT (MVCT) images for dose recomputations. Phys Med Biol 2005;50:4259–76.
[26] Stützel J, Oelfke U, Nill S. A quantitative image quality comparison of four different image guided radiotherapy devices. Radiother Oncol 2008;86:20–4.
[27] Branchini M, Fiorino C, Dell'Oca I, Belli ML, Perna L, Di Muzio N, et al. Validation of

a method for “dose of the day” calculation in head-neck tomotherapy by using planning ct-to-MVCT deformable image registration. Phys Med 2017;39:73–9.
[28] Broggi S, Perna L, Bonsignore F, Rinaldin G, Fiorino C, Chiara A, et al. Static and rotational intensity modulated techniques for head-neck cancer radiotherapy: a planning comparison. Phys Med 2014;30:973–9.
[29] Fiorino C, Dell’Oca I, Pierelli A, Broggi S, Cattaneo GM, Chiara A, et al. Simultaneous Integrated Boost (SIB) for nasopharynx cancer with helical tomotherapy, a planning study. Strahlenther Onkol 2007;183:497–505.
[30] Lu W, Olivera GH, Chen Q, Ruchala KJ, Haimerl J, Meeks SL, et al. Deformable registration of the planning image (kVCT) and the daily images (MVCT) for adaptive radiation therapy. Phys Med Biol 2006;51:4357–74.
[31] Fedorov A, Beichel R, Kalpathy-Cramer J, Finet J, Fillion-Robin JC, Pujol S, et al. 3D Slicer as an image computing platform for the Quantitative Imaging Network. Magn Reson Imag 2012;30:1323–41.
[32] Kirby N, Chuang C, Ueda U, Pouliot J. The need for application-based adaptation of deformable image registration. Med Phys 2013;40:011702.
[33] Piper J. SU-FF-I-68: evaluation of an intensity-based free-form deformable registration algorithm. Med Phys 2007;34:2353–4.
[34] Piper J. Evaluation of a CT to Cone-Beam CT Deformable Registration Algorithm. Proceedings of the 49th annual ASTRO meeting. Int J Radiat Oncol Biol Phys. 2007. p. S418–9.
[35] Low DA, Harms WB, Mutic S, Purdy JA. A technique for the quantitative evaluation of dose distributions. Med Phys 1998;25:656–61.
[36] Pinter C, Lasso A, Wang A, Jaffray D, Fichtinger G. SlicerRT: radiation therapy research toolkit for 3D Slicer. Med Phys 2012;39:6332–8.
[37] Martens C, Reynaert N, De Wagter C, Nilsson P, Coghe M, Palmans H, et al. Underdosage of the upper-airway mucosa for small fields as used in intensity-modulated radiation therapy: a comparison between radiochromic film measurements, Monte Carlo simulations, and collapsed cone convolution. Med Phys 2002;29:1528–35.
[38] Ardu V, Broggi S, Cattaneo GM, Mangili P, Calandrino R. Dosimetric accuracy of tomotherapy dose calculation in thorax lesions. Radiat Oncol 2011;6:14.
[39] Zhao Y, Mackenzie M, Kirby C, Fallone BG. Monte Carlo evaluation of treatment planning system for tomotherapy in an anthropomorphic heterogeneous phantom and for clinical treatment plans. Med Phys 2008;35:5366–74.
[40] Sterpin E, Salvat F, Olivera G, Vynckier S. Monte Carlo evaluation of the convolution/superposition algorithm of hi-art tomotherapy in heterogeneous phantoms and clinical cases. Med Phys 2009;36:1566–75.
[41] Zani M, Talamonti C, Bucciolini M, Marinelli M, Verona-Rinati G, Bonomo P, et al. In phantom assessment of superficial doses under TomoTherapy irradiation. Phys Med 2016;32:1263–70.
[42] Ramsey CR, Seibert RM, Robison B, Mitchell M. Helical tomotherapy superficial dose measurements. Med Phys 2007;34:3286–93.
[43] Cheek D, Gibbons JP, Rosen II, Hogstrom KR. Accuracy of TomoTherapy treatments for superficial target volumes. Med Phys 2008;35:3565–73.
[44] Javedan K, Zhang G, Mueller R, Harris E, Berk L, Forster K. Skin dose study of chest wall treatment with tomotherapy. Jpn J Radiol 2009;27:355–62.
[45] Hardcastle N, Soisson E, Metcalfe P, Rosenfeld AB, Tome WA. Dosimetric verification of helical tomotherapy for total scalp irradiation. Med Phys 2008;35:5061–8.
[46] Avanzo M, Drigo A, Ren Kaiser S, Roggio A, Sartor G, Chiovati P, et al. Dose to the skin in helical tomotherapy: results of in vivo measurements with radiochromic films. Phys Med 2013;29:304–11.
[47] Tournel K, Verellen D, Duchateau M, Fierens Y, Linthout N, Reynders T, et al. An assessment of the use of skin flashes in helical tomotherapy using phantom and in-vivo dosimetry. Radiother Oncol 2007;84:34–9.